COBEM 2023 27TH INTERNATIONAL CONGRESS OF MECHANICAL ENGINEERING

ABCM Brazilian Society of Mechanical Sciences and Engineering
27th ABCM International Congress of Mechanical Engineering
December 04-08, 2023, Florianópolis-SC, Brazil

COB-2023-0370
INFLUENCE OF GRAPHENE ON THE RHEOLOGICAL PROPERTIES OF WAXY OIL

Rufino Kussima Agostinho Epesse
Diogo Elias da Vinha Andrade
Rheology and Non-Newtonian Fluid Flow Laboratory - ReoSul, Graduate Program in Mechanical Engineering – PROMEC, Federal University of Rio Grande do Sul -UFRGS, Brazil
rufinopagliarin@gmail.com, diogo.andrade@ufrgs.br

Cezar Otaviano Ribeiro Negrão
Géssica Palaoro
Research Center for Rheology and Non-Newtonian Fluids—CERNN, Postgraduate Program in Mechanical and Materials Engineering—PPGEM, Federal University of Technology-Paraná—UTFPR
negrao@utfpr.edu.br, palaorogessica@gmail.com

Ricardo Jorge Espanhol Andrade
Nathália Maria Moraes Fernandes
Engineering School, Mackenzie Presbyterian University, Sãao Paulo, Brazil
MackGraphe - Mackenzie Institute for Research in Graphene and Nanotechnologies, São Paulo, Brazil
ricardo.andrade@mackenzie.br, nathalia.m.moraes@hotmail.com

Abstract. *In the reservoir, waxy crude oils are subjected to high pressures and high temperatures. In this condition, the hydrocarbons, which are the main components of crude oil, are dissolved in the liquid phase. During the production and transportation of the oil, the pipelines are in contact with the seafloor which is around 4 ºC. At low temperatures, the solubility of high molecular weight components in the oil decreases and the n-paraffins tend to precipitate as crystal structures. Wax crystallization not only increases considerably the oil viscosity but also provides a solid-like structure to the material when the flow is interrupted. In these cases, high pressures are required to break up the gelled structure and consequently, to restart the flow. Different methods have been proposed in the literature to reduce the oil viscosity and the material yield stress. In the current study, the influence of graphene nanoparticles on the rheological properties of model waxy oils was investigated. The analysis was performed by using a rotational rheometer in which the thermal and shear histories of the sample were controlled. Viscoelastic response, apparent viscosity, and yield stress of the model waxy oils samples with nanoparticles and without nanoparticles were measured and compared. It was observed that in the presence of graphene, the crystallization temperature dropped from 33°C to 13°C. The dynamic viscosity at the final cooling temperature changed from 1.44 to 0.084 Pa.s with the graphene addition. With the inclusion of graphene, the critical stress, or the yield stress (both dynamic and static), decreased to zero. These results show that the addition of graphene nanoparticles significantly impacted the rheological behavior of the formulated paraffinic oils, leading to a reduced crystallization temperature, yield stress, and apparent viscosity.*

Keywords: *graphene, waxy oil, rheology, yield stress*

1. INTRODUCTION

Crude oil is a complex mixture of hydrocarbons, which contains paraffins, asphaltenes, resins, aromatics, and naphthenes. Among these components, asphaltenes and paraffins are recognized to create significant challenges in oil production and transportation facilities (Ansaroudi et al., 2013).

The overwhelming majority of crude oils and their products contain substantial amounts of waxes also known as paraffin. Paraffins are mixtures of hydrocarbons consisting of linear or normal chains, typically comprising 20 to 40 carbon atoms, as well as alkanes with branched and cyclic chains. Paraffin crystals precipitate and grow as temperature decreases, creating a crystalline network, which begins to trap the molecules of liquid hydrocarbon until the oil cannot flow. The temperature at which this happens is called pour point or gelation temperature (Taraneh et al., 2008). Paraffin deposition negatively impacts the production and transportation of oil and its derivatives, leading to decreased output and higher operational expenses, as well as creating handling difficulties in regions where the service temperatures are very low.

The flow characteristics of waxy crude oil under low temperature conditions can be enhanced through the application of wax control chemicals, such as pour point depressants (PPDs) (Taraneh et al., 2008; Jia et al., 2022; Mahmoud and Betiha, 2021). Treatment of waxy crude oils with effective PPDs results in lower pour points, viscosities, and yield

stresses compared to untreated oils. These PPDs act to modify the wax crystal formation and inhibit their agglomeration, thereby improving flowability and reducing the risks of flow restrictions and operational challenges during oil production and transportation.

Due to features such as unique size, quantum tunneling, and high adsorption power, nanoparticles offer significant potential in modifying conventional polymeric PPDs (Yang et al., 2015; Hao et al., 2019). In light of recent advances in nanotechnology, new developments have emerged, such as nanohybrid PPDs that are combinations of nanomaterials and traditional PPDs (Ragunathan et al., 2020). Some researchers suggest several possible mechanisms that might explain the enhanced performance related to nanohybrid PPDs: (1) changes in nucleation, where nanoparticles serve as dispersed nucleation points; (2) co-crystallization, which involves the integration of nanoparticles into wax crystals, limiting their growth; and (3) adsorption of nanoparticles on the surface of wax crystals, modulating their growth (Wang et al., 2011).

The objective of this study is to evaluate the rheological properties of model waxy oils in the presence of graphene. For this purpose, rheometric tests were conducted, and the analyses and hypotheses were formulated based on the results obtained from the tests.

2. MATERIALS AND METHODS

2.1 Material

The experimental investigation was conducted using a model waxy oil composed of 90 wt % of transparent mineral oil (Sigma Aldrich-330779) and 10 wt % of white paraffin wax with a melting point between 58 and 62 °C (Sigma Aldrich-327212); the same wax and mineral oil that have been used in recent works (Legnani et al., 2020; Dimitriou et al., 2011; Andrade et al., 2017; Andrade et al., 2018; Andrade et al., 2020; Mendes et al., 2017). Additionally, graphene nanoparticles were added to the model waxy oil to obtain a suspension with a graphene mass concentration of 0.01 wt %.

The rheological tests were performed using the Anton Paar MCR 502 rotational rheometer (Figure 1). The temperature of the rheometer base was controlled using a Peltier electronic system with the assistance of a thermostatic bath. For the experiments, grooved parallel plates geometries with a diameter of 40 mm and a 1mm-gap were used.

Figure 1. Anton Paar MCR 502 rotational rheometer.

2.2 Apparatus and tests procedure

The preparation of the model waxy oil samples involved the following procedures: i) addition of 10 wt % of paraffin wax to 90 wt % of mineral oil in a hermetically sealed container; ii) placing the mixture in a thermal oven at 60 °C for 1 hour to ensure complete dissolution of the paraffin wax.

For the formulation of the model waxy oil with graphene, the procedure was as follows: i) preparation of the waxy oil sample as described earlier; ii) weighing the mass fraction of graphene into the waxy oil sample iii) placing the sample (in a closed container) in an ultrasonic bath with a frequency of 35 kHz and power of 50 W for 4 hours to defragment and disperse the nanoparticles, reducing agglomerations and improving stability. The graphene dispersion was performed at 60 °C to prevent the wax precipitation during this process. Figure 2 shows the samples without graphene and with graphene at high temperature after preparation.

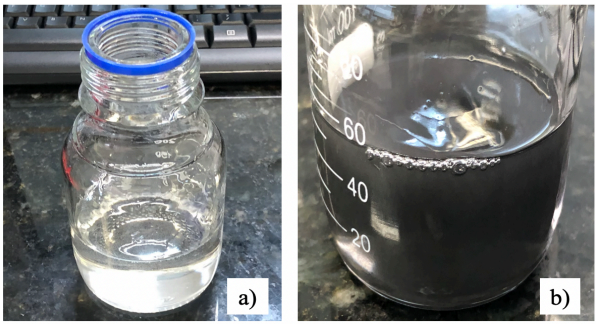

Figure 2. Samples at high temperature after preparation. a) Sample of 10 wt % paraffin wax in oil and b) original sample with the addition of 0.01 wt % graphene.

In order to evaluate the influence of graphene nanoparticles on the rheological behavior of model waxy oil, several rheometric tests were conducted. To improve repeatability and facilitate comparison between results, a pre-test procedure was implemented, which consisted of the following steps:

i. Place a syringe containing the sample in the oven at 60 °C for 30 minutes to completely dissolve the paraffin wax in the oil.

ii. Preheat the rheometer to the initial test temperature (50 °C).

iii. Transfer the sample to the rheometer using the preheated syringe. Figure 3 shows the process of transferring the sample to the rheometer using a syringe.

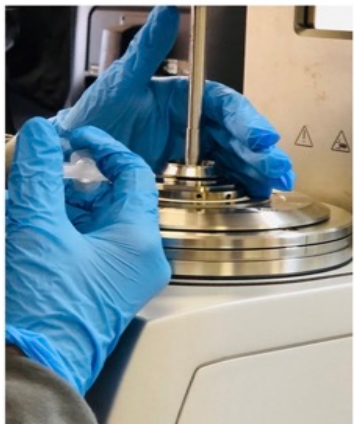

Figure 3. Process of transferring the sample to the preheated rheometer with grooved parallel plates geometries, using a syringe.

iv. For the oil samples with graphene, prior to the tests, they underwent a homogenization process in an ultrasonic bath for 30 minutes at 60 °C. This step was performed to ensure a uniform dispersion of the graphene in the samples. Figure 4 illustrates the ultrasonic bath containing the samples with graphene during the homogenization process.

Rheological tests were conducted under two distinct cooling methods: dynamic and static cooling. During dynamic cooling, the sample underwent a strain rate of 10 s^{-1} while being cooled at a rate of 1°C/min from 50°C to 4°C. Throughout this process, apparent viscosity was continuously monitored as a function of the decreasing temperature. Subsequently, a stress ramp ranging from 0.1 Pa to 100 Pa was imposed to determine the critical flow stress for flow restart. To prevent the rheometer from exceeding its maximum rotation, the stress ramp is interrupted at the moment the shear rate reaches 100 s^{-1}. After the stress ramp, the shear rate was reduced from 350 s^{-1} down to 1 s^{-1} to obtain the flow curve. In the static cooling approach, the sample was first cooled at rest. During this cooling approach, an oscillatory test with low strain amplitude was conducted to determine the gelation temperature, denoted by T_g. After reaching the desired cooled state, the sample was left undisturbed for 10 minutes. Following this, a stress ramp ranging from 0.001 Pa to 10.000 Pa was implemented, aiming to identify the critical stress required to start up the flow after the static cooling. In this stress ramp the test is finished at the moment the shear rate reaches 100 s^{-1}.

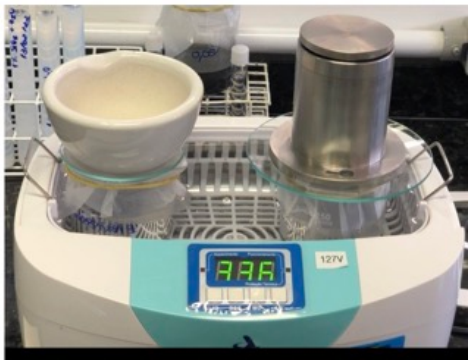

Figure 4. Process of homogenizing the sample with graphene in an ultrasonic bath for 30 minutes at 60 °C.

.

3. RESULTS AND DISCUSSION

3.1 Effect of graphene on the viscosity of waxy oil

After a 30 minute period at the initial temperature, the tested sample was dynamically cooled from 50 to 4 °C with a cooling rate of 1°C/min and a constant shear rate of 10 s^{-1}. Figure 5 illustrates the relationship between dynamic viscosity and temperature for the waxy oil sample (W.O.) and the waxy oil sample with the addition of graphene (W.O. + graphene). In Figure 5 (a), it is evident the viscosity of the samples increases as the temperature decreases. Moreover, both the (W.O.) and (W.O. + graphene) samples exhibit similar viscosity values until approximately 33°C. To describe the relationship between dynamic viscosity and temperature, the Arrhenius type equation can be employed:

$$\mu_d = \mu_{ref} e^{\frac{\Delta H}{R}\left(\frac{1}{T}-\frac{1}{T_{ref}}\right)} \quad (1)$$

where μ_{ref} is the dynamic viscosity of the fluid at a reference temperature T_{ref}, R is the universal gas constant, and ΔH is the activation energy for flow.

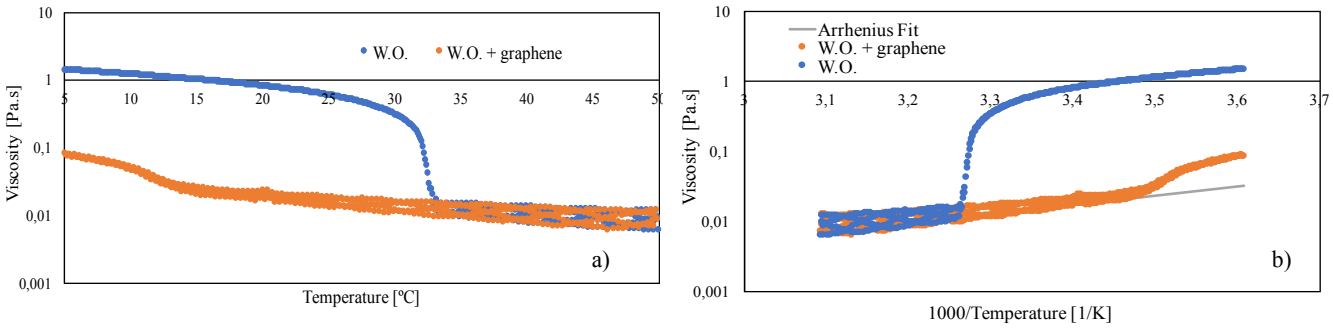

Figure 5. Viscosity of waxy oil sample as a function of temperature with a cooling rate of 1°C/min and a constant shear rate of 10 s^{-1}. a) Experimental viscosity as a function of temperature b) Experimental viscosity as a function of the inverse of temperature and fit to the Arrhenius type equation with μ_{ref} (50 °C) = 0,0067 Pa.s and ΔH/R = 3000 K.

In Figure 5 (b), the comparison between the viscosity values obtained from the Arrhenius equation fitting and the experimental values from Figure 5 (a) is presented. It is notable that the Arrhenius equation successfully predicts the viscosity behavior for both samples until a certain point. Beyond this point, the presence of precipitated crystals in the solution starts to influence the material's behavior. This critical point, characterized by a significant change in dynamic viscosity, is referred to as the crystallization temperature T_c in this study.

With the addition of graphene to the waxy oil sample, the crystallization temperature decreased drastically. The reduction was from 33 to 13°C when comparing the samples without and with graphene, respectively. The viscosity at the final cooling temperature (i.e., 4°C) significantly decreased with the addition of graphene to the waxy oil sample, from 1.44 to 0.084 Pa.s.

3.2 Influence of graphene on the critical stress of waxy oil (dynamic cooling)

Figure 6 illustrates the strain responses as a function of shear stress for the tests conducted on the waxy oil sample without graphene and the waxy oil sample with graphene.

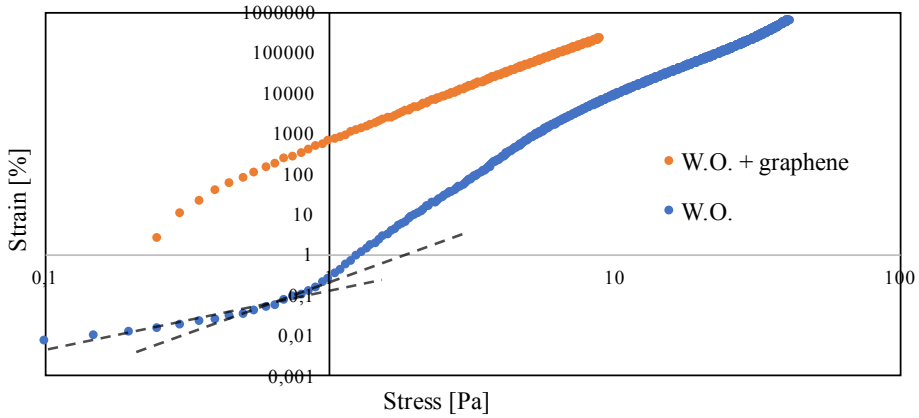

Figure 6. Strain as a function of stress for the shear stress ramp test with waxy oil sample.

It is observed that at low stresses, in the predominantly elastic region, the material with graphene exhibits much higher strain values for the same stresses. In the sample without graphene, at a certain point, the material's structure collapses, and the strain increases abruptly. Therefore, the yield point was determined by the intersection of two lines near the inflection region of the strain curve. These lines were drawn immediately before and after this region. For the waxy oil sample without graphene, the corresponding critical stress value was approximately 0.6 Pa. In contrast, for the waxy oil sample with graphene, the critical stress was practically zero since there was no abrupt increase in strain. The reduction was from 0.6 Pa to zero when comparing the samples without and with graphene, respectively.

3.3 Time-dependent response and flow curve

The step-strain rate tests were conducted with the following parameters: shear rates of 350; 300; 100; 30; 10; 3; and 1 s^{-1} , and step durations of 1200 s. Figure 7 shows the control of shear rate and shear stress measurements as a function of time for waxy oil sample without graphene and with graphene.

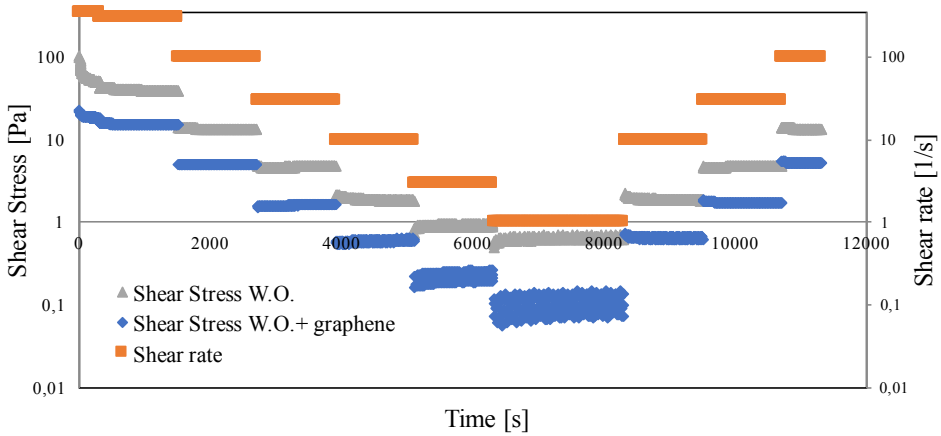

Figure 7. Shear stress as a function of time for different imposed shear rate. Test performed at 4 ◦C after a dynamic cooling of 50 ◦C to 4 ◦C, cooling rate of 1.0 ◦C /min and shear rate of 10 s^{-1}during the cooling.

It is noted that when imposing a shear rate of 350 s^{-1} for the first 300 s, there is a decrease in shear stress, and the steady-state regime is not reached. The same occurs when imposing a shear rate of 300 s^{-1}. However, when imposing the third step of shear rate (100 s^{-1} for 1200 s), the waxy oil sample reaches equilibrium almost immediately, at approximately 2700 s of testing. The steady-state regime is achieved for the shear rates of 30; 10; 3; and 1 s^{-1}, which provide data points for the flow curve. Figure 8 shows the experimental results gathered for steady-state shear stress as a function of the strain rate. The data points were fitted using the Bingham equation for the sample without graphene and by the power-law equation for the sample with graphene. The fitted curves are represented by dashed lines.

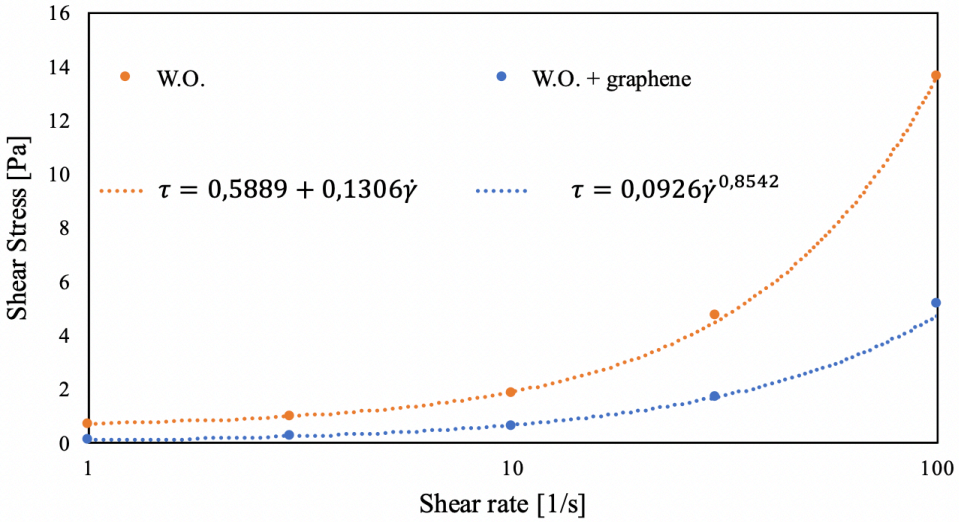

Figure 8. Shear stress as a function of shear rate obtained by reducing the shear rate from 350 to 1 s^{-1} . The points represent the final value of each shear rate plateau presented in Figure 7.

It can be observed that the linear coefficient, which is the point where the line intersects the ordinate axis, indicates the dynamic yield stress, which is $\tau_y = 0.5889$ Pa for waxy oil sample without graphene. For the waxy oil sample with graphene, the yield stress can be considered as zero. The yield stress values are closely aligned with the critical stresses observed in the stress ramp tests as illustrated in Figure 6. The plastic viscosity is the slope of the fitted line, which is $\mu = 0.1306$ Pa. s for waxy oil sample without graphene. For the for waxy oil sample with graphene, the consistency index of the power-law model is $m = 0.0926$. $\dot{\gamma}$ is the imposed strain rate, measured in s^{-1}, and $n = 0.8542$ is the power-law index for the waxy oil sample with graphene. Notably, when graphene is present, the dynamic yield stress reduces to zero.

3.4 Low amplitude oscillatory shear test

Oscillatory tests were carried out at a constant frequency of 1 Hz. For the sample without graphene, a strain amplitude of 10^{-5} was employed, as illustrated in Figure 9a. For the sample containing graphene, the strain amplitude was set to 10^{-2}, as illustrated in Figure 9b.

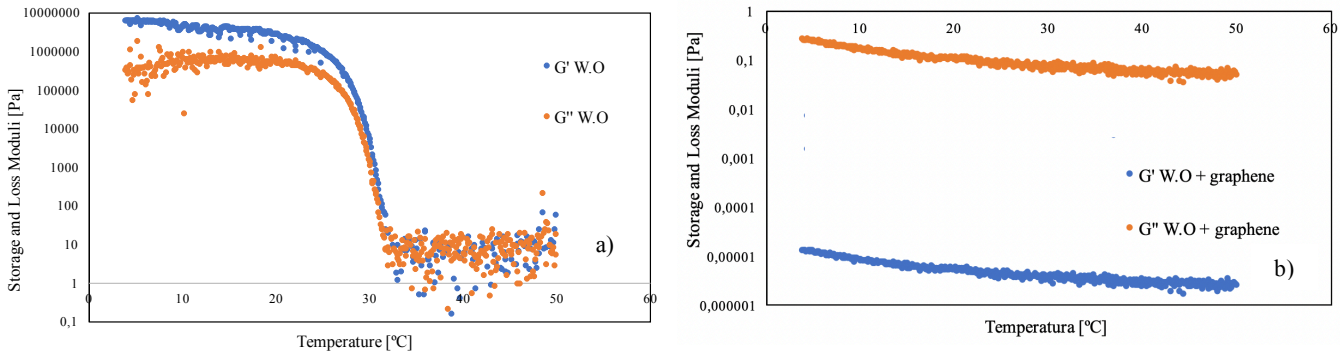

Figure 9. Evolution of storage and loss moduli over time. a) Sample without graphene at a constant strain amplitude of 10^{-5}; b) Sample with graphene at a constant strain amplitude of 10^{-2}.

It can be observed that the sample without added graphene (Figure 9a) indicates that, at elevated temperatures, the dynamic moduli are nearly equivalent, implying a balance between the viscous and elastic properties of the material. At a critical temperature of 31°C, a transition occurs wherein the storage modulus (G') starts to exceed the loss modulus (G"), indicating a rise in the elastic behavior. At lower temperatures, G' remains higher than G", reinforcing the material's predominantly elastic nature. In contrast, for the sample with graphene (Figure 5b), the G" module consistently surpassed G' across the entire temperature range assessed, suggesting a predominantly viscous behavior. Additionally, it's noteworthy that the transition temperature, where G' starts to exceed G" for the sample without graphene, is lower compared to the point of significant variation in dynamic viscosity for the waxy oil sample without graphene, as depicted in Figure 1.

It's crucial to note that both strain amplitudes lie within the linear viscoelasticity region for the materials studied. For the waxy oil sample without graphene, when the strain exceeds 10^{-4}, the material reaches the non-linear regime as

presented in a previous paper (Andrade and Coussot 2019). In this region, the relationship between stress and strain is no longer directly proportional, potentially leading to phenomena like strain-induced microstructure changes. These changes can obscure the accurate interpretation of the test results. In contrast, as the sample with graphene did not reach the structured condition, in this sample strains smaller than 10^{-2} might be below the rheometer's torque detection threshold. This suggests that the readings might lack precision; in certain instances, the device might not even detect a discernible reaction from the material. Additionally, the instrument's response signal could blend with its intrinsic noise level, rendering the acquired data less reliable. The same behavior that is observed in the sample without graphene at temperature higher than the gelation point as can be seen in Figure 1(a).

3.5 Influence of graphene on the critical stress of waxy oil (Static yield stress)

A stress ramp was applied with the aim of determining the critical stress to restart flow. The strain results as a function of the shear stress for tests with waxy oil sample, both without and with graphene, are presented in Figure 10.

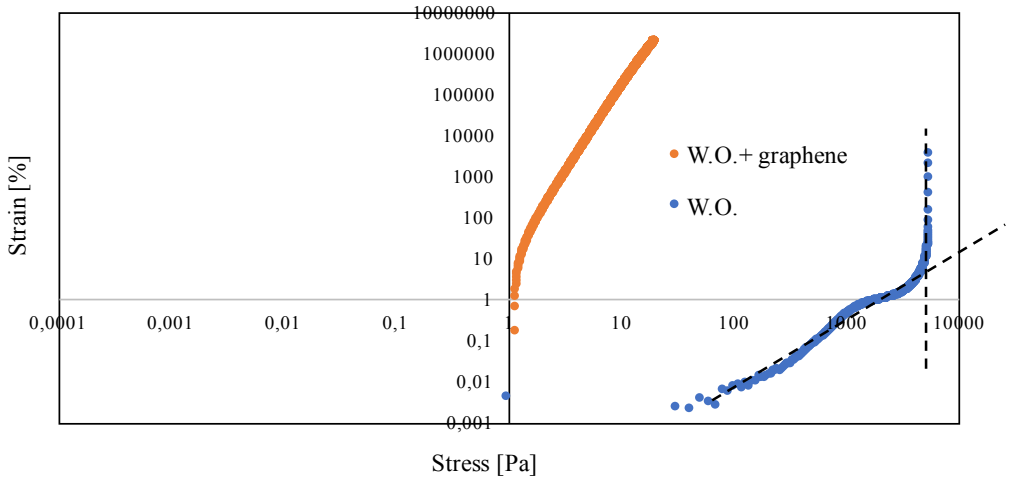

Figure 10. Strain as a function of stress for the shear stress ramp test with waxy oil sample.

It can be observed that in the primarily elastic region, the material demonstrates minimal strain under low stresses. For the sample without graphene (blue curve), there's a point where the material undergoes a sudden increase in strain, indicating a structural collapse. This yield point is identified near the strain curve's inflection, marked by the intersection of two lines drawn immediately before and after this point. The critical stress value for the waxy oil sample without graphene was around 4500 Pa. However, in the sample with graphene, there's essentially no critical stress, as there wasn't a sudden strain increase. Thus, comparing the two samples, the stress value went from 4500 Pa to nearly zero.

4. CONCLUSION

In the current study, the influence of graphene nanoparticles on the rheological properties of model waxy oils was investigated. The analysis was performed by using a rotational rheometer in which the thermal and shear histories of the sample were controlled. Viscoelastic response, apparent viscosity, and yield stress of the model waxy oils samples with nanoparticles and without nanoparticles were measured. It was observed that in the presence of graphene, the crystallization temperature dropped from 33°C to 13°C. The dynamic viscosity at the final cooling temperature (i.e., 4°C) for the waxy oil sample without graphene was 1.44 Pa.s, while for the waxy oil sample with graphene, it was 0.084 Pa.s. With the inclusion of graphene, the critical stress, or the yield stress (both dynamic and static), decreased to zero.

These results suggest that the addition of graphene nanoparticles significantly impacted the rheological behavior of the formulated paraffinic oils, leading to a reduced crystallization temperature, yield stress, and apparent viscosity.

5. ACKNOWLEDGEMENTS

The authors thanks CNPq for grants 406765/2022-7 (INCT-Rhe9 - National Institute of Science and Technology for Rheology of Complex Materials Applied to Advanced Technologies), 305109/2022-7 and 405200/2021-8 for the financial support. This work has been partially funded by the Brazilian agency CAPES (PROEX). Epesse R.K.A. would like to express his gratitude to the National Institute for Scholarship Management of Angola (INAGBE) for providing him with a master's scholarship, and to the Postgraduate Program in Mechanical Engineering at the Federal University of Rio Grande do Sul (PROMEC) for the funding that enabled him to conduct the tests in Curitiba, at the Federal University of Technology-Paraná.

6. REFERENCES

Andrade, D.E.V., Coussot, P., 2019. "Brittle solid collapse to simple liquid for a waxy suspension". *Soft Matter,* vol. 15, n. 43, p. 8766-8777.

Andrade, D.E.V., Neto, M.A.M., Negrão, C.O.R., 2017. "The importance of supersaturation on determining the solid-liquid equilibrium temperature of waxy oils". *Fuel*, vol. 206, p. 516-523.

Andrade, D.E.V., Neto, M.A.M., Negrão, C.O.R., 2018. "Non-monotonic response of waxy oil gel strength to cooling rate". *Rheologica Acta*, vol. 57, p. 673-680.

Andrade, D.E.V., Ferrari, M., Coussot, P., 2020. "The liquid regime of waxy oils suspensions: a Magnetic Resonance Velocimetry Analysis". *Journal of Non-Newtonian Fluid Mechanics*, vol. 279, p. 104261.

Ansaroudi, H.R.J., Vafaie-Sefti, M., Masoudi, Sh., Behbahani, T.J., Jafari, H., 2013. "Study of the Morphology of Wax Crystals in the Presence of Ethylene-co-vinyl Acetate Copolymer". *Petroleum Science and Technology*, vol. 31, n. 6, p. 643-651.

Dimitriou, J., McKinley, H., Venkatesan, R., 2011. "Rheo-PIV analysis of the yielding and flow of model waxy crude oils". *Energy & Fuels*, vol. 25, n. 7, p. 3040-3052.

Hao, L.Z., Al-Salim, H. S., Ridzuan, N., 2019. "A Review of the Mechanism and Role of Wax Inhibitors in the Wax Deposition and Precipitation". *Pertanika Journal of Science & Technology*, vol. 27, n. 1.

Jia X., Fu M., Xing X., Wei L., Song Y., Zhang L., Geng X., Guo H., 2022. "Submicron carbon-based hybrid nano-pour-point depressant with outstanding pour point depressant and excellent viscosity depressant". *Arabian Journal of Chemistry*, vol. 15, n. 10, p. 104157.

Legnani, A., Santos, T.G.M., Andrade, D. E.V., Negrão, C.O.R., 2020. "Waxy oils: Deformation-dependent materials". *Journal of Non-Newtonian Fluid Mechanics*, vol. 285, p. 104378.

Mahmoud T., Betiha M.A., 2021. "Poly(octadecyl acrylate-co-vinyl neodecanoate)/Oleic Acid-Modified Nano-graphene Oxide as a Pour Point Depressant and an Enhancer of Waxy Oil Transportation". *Energy & Fuels*, vol. 35, n. 7, p. 6101-6112.

Mendes, R., Vinay, G., Ovarlez, G., Coussot, P., 2015. "Reversible and irreversible destructuring flow in waxy oils: an MRI study, J. Non – Newton". *Journal of Non-Newtonian Fluid Mechanics*, vol. 220, p. 77-86.

Ragunathan, T., Husin, H., Wood, C. D., 2020. "Wax formation mechanisms, wax chemical inhibitors and factors affecting chemical inhibition". *Applied sciences*, vol. 10, n. 2, p. 479.

Taraneh, J.B., Rahmatollah, G., Hassan, A., Alireza, D., 2008. "Effect of wax inhibitors on pour point and rheological properties of Iranian waxy crude oil". *Fuel processing technology*, vol. 89, n. 10, p. 973-977.

Wang, F. et al., 2011. "The effect of nanohybrid materials on the pour-point and viscosity depressing of waxy crude oil". *Chinese science bulletin*, vol. 56, p. 14-17.

Yang, F. et al., 2015. "Polymeric wax inhibitors and pour point depressants for waxy crude oils: a critical review". *Journal of Dispersion Science and Technology*, vol. 36, n. 2, p. 213-225.

7. RESPONSIBILITY NOTICE

The authors are the only responsible for the printed material included in this paper.